Study of Thermal Phase Transitions in Iota Carrageenan Gels via Fluorescence Technique

Özlem Tari,[1] Selim Kara,[2] Önder Pekcan[3]

[1]*Department of Physics, Istanbul Technical University, Maslak, Istanbul 34469, Turkey*
[2]*Department of Physics, Trakya University, Edirne 22030, Turkey*
[3]*School of Arts and Sciences, Kadir Has University, Cibali, Istanbul 34083, Turkey*

Received 25 March 2009; accepted 3 August 2009
DOI 10.1002/app.31233
Published online 29 March 2011 in Wiley Online Library (wileyonlinelibrary.com).

ABSTRACT: The effect of carrageenan concentration on thermal phase transitions of the iota carrageenan gels was investigated by using fluorescence technique. During heating and cooling processes, scattered light, I_{sc}, and fluorescence intensity, I_p, were monitored against temperature to investigate phase transitions. Transition temperatures from the derivative of the transition paths were determined. Two regions were observed during the heating and cooling processes. At the first step of the heating, dimers were converted into double helix by undergoing dimer to double helix (d-h) transition. At the higher temperature region, double helix to coil (h-c) transition took place. During the cooling process, these transitions are arranged in the order of coil to double helix (c-h) and double helix to dimer (h-d). A hysteresis was observed between (h-d) and (d-h) transitions. The critical gel fraction exponents, β, were found to be independent of the system by indicating that they all fall into the same universality class. © 2011 Wiley Periodicals, Inc. J Appl Polym Sci 121: 2652–2661, 2011

Key words: fluorescence; gels; transitions

INTRODUCTION

Carrageenan is one of the key products in the seaweed polysaccharide industry.[1] It is obtained from Rhodophyceas (red seaweed) by extraction. Carrageenan is a large molecule made up of some 1000 galactose residues with three main types: Kappa, Iota, and Lambda according to the relative number and position of sulfate ester substituents. They are very important in many technological applications, especially in cosmetics, pharmaceuticals, and personal care industries.[2] In cosmetic applications, preserving moisture in hand lotions is quite important for keeping skin softer. In pharmaceutical industry, they are used for the design of slow-release devices for oral drugs.

ι-carrageenan is the most highly sulfated of the helix-forming polysaccharides, which has a high molecular weight linear polymer consisting principally of an alternating sequence of 3-linked β-D-galactose 4-sulfate and 4-linked 3,6-anhydro-β-D-galactose 2-sulfate. Thus, each monosaccharide unit in the ideal polysaccharide carries one sulfate group, and therefore ι-carrageenan behaves in aqueous solution as a highly charged polyanion in the extended confirmation.[3] It is known that the polysaccharide has a double helix conformation in the solid phase by X-ray Diffraction data while in calcium salt it is converted to a three-fold right-handed double helix with parallel strands.[4–6] In solution, ι-carrageenan is reversibly transformed from an ordered to a disordered conformation. Naturally at high ionic strength and low temperature ι-carrageenan forms an ordered state. Upon heating, the helices dissolve and the ι-carrageenan forms a random coil conformation.[7] Intermolecular double helix formation investigated by several groups should result in a doubling in the observed molecular weight of the ι-carrageenan.[8,9] However, some authors have proposed monomolecular single-helix formations.[10]

The kinetics and equilibrium processes of the sol–gel and gel–sol transitions of agar or agarose gels as well as the effect of gelation conditions on gel's microstructure and rheological properties have been studied in last few years.[11–13] It was observed that gelation of agar molecules results in a large sigmoidal increase in the magnitude of the sol's shear modulus.[14,15] On reheating, the gel structure is destroyed and during the gel–sol transition, the shear modulus follows another sigmoidal path back to its initial value, forming a hysteresis loop.[16] The observed values of the sol–gel and gel–sol temperatures found in this study are 36°C and 78°C, respectively. It was understood that the sol–gel and gel–sol temperatures can be affected by the agar concentration and the thermal history of the gel. Cation effect on sol–gel and gel–sol phase transitions of κ-carrageenan was

Correspondence to: Ö. Pekcan (pekcan@khas.edu.tr).

studied by using photon transmission technique.[17] Similar technique was also employed to investigate the hysteresis during sol–gel and gel–sol transitions in κ-carrageenan-water system.[18] Recently, fluorescence technique was used to study thermal phase transitions of κ-carrageenan in various salt solutions.[19,20]

In this study, phase transitions of iota carrageenan in various concentrations were studied using fluorescence technique. Pyranine (P) (a derivative of pyrene molecule) was used as fluorescence probe. Scattered light, I_{sc} and fluorescence intensity, I_p were monitored against temperature to determine phase transitions and transition temperatures. The necessary correction on the pyranine intensity was made to produce the real transition curves. The gel fraction exponent β was calculated and found to be in accord with the classical Flory-Stockmayer Model.

THEORETICAL CONSIDERATIONS

For the critical exponents (γ and β) near the sol–gel phase transition, classical theories like those of the Flory-Stockmayer predict one set of exponents, whereas scaling theories based on lattice percolation predict different exponents. The two groups of theories differ in their treatment of intramolecular loops, space dimensionality, and excluded volume effects. Historically, the exact solution of the sol–gel transition was first given by Flory and Stockmayer on a special lattice called the Bethe lattice on which the closed loops were ignored. The exponents γ and β for the weight average degree of polymerization, DP_w, and the gel fraction G both are equal to unity, independent of the dimensionality in the Flory-Stockmayer model, which is also called classical theory or kinetic theory.[21,22] An alternative to this model is the lattice percolation model where monomers are thought to occupy the sites of a periodic lattice.[23–25] A bond between these lattice sites is formed randomly with probability P. At a certain bond concentration p_c, defined as the percolation threshold, the infinite cluster is formed in the thermodynamic limit. This is called the gel in polymer language. The polymeric system is in the sol state below the critical conversion, p_c.

The predictions of these two theories about the critical exponents for the sol–gel transition are different from the point of the universality. Consider, for example the exponents γ and β for the weight average degree of polymerization, DP_w, and the gel fraction G, (average cluster size S_{av}, and the strength of the infinite network P_∞, in percolation language) near the gel point, are defined as:

$$DP_w \propto (p_c - p)^{-\gamma}, \qquad p \to p_c^- \tag{1}$$

$$G \propto (p - p_c)^{\beta}, \qquad p \to p_c^+ \tag{2}$$

where the Flory-Stockmayer theory gives $\beta = 1$ and $\gamma = 1$, independent of the dimensionality, while the percolation studies (using series expansions or computer simulations) give γ and β around 1.80 and 0.41 in three dimension.[24,25]

Some realistic features like multiple bonding, reversibility, and effect of solvent are generally not considered in static percolation, while the closed loops are ignored in Flory-Stockmayer theory. There are much more developments in the sol–gel modeling beyond static percolation. In literature,[26,27] some kinetics are included to make the sol–gel kinetics different from static percolation. By the computer simulation studies, Liu and Pandey showed that the exponents γ and β change considerably for various solvent conditions, i.e., reversibility for physical gels and the quality of solvent do effect the sol–gel transition.[28] They also argued that the sol–gel transition for chemical gelation seems also nonuniversal with respect to quality of the solvent and rate of reaction due to the interplay between the phase separation and crosslinking.[29]

To understand the physical nature of polymerization processes underlying the transitions from the sol to the gel state, one must follow the reaction kinetics, compare results with experiments directly measuring some physical properties in the course of the polymerization reaction. Experimental techniques used for monitoring this transition should be very sensitive to the structural changes, and should not disturb the system mechanically. Fluorescence technique is particularly useful for studying the detailed structural aspects of the gels. The fluorescence technique is based on the interpretation of the change in anisotropy, emission and/or excitation spectra, emission intensity, and viewing the lifetimes of embedded dye molecules to monitor the change in their microenvironment.[30,31] It can be used in two ways for the studies on polymerization and gelation. First, one can add a fluorescence dye as a free probe to the system. By using fluorescence probe it is possible to determine the microenvironment (polarity, viscosity, etc.) within the gel. In the second approach, the fluorescence dye is covalently attached to the polymer, and serves as a polymer-bond label.

In this study, one can argue that the total fluorescence intensity from the pyranines monitors the average degree of polymerization and the growing gel fraction, far below and above the gel point, respectively. This proportionality can easily be shown by using a Stauffer type argument as follow under the assumption that the monomers from the sites of a periodic lattice.[24]

The probability that a site belongs to a cluster of size s is given by $n_s s$ where n is the number of s-cluster (number of clusters including s sites) per lattice site. The probability that an arbitrary site belongs to any cluster is P, which is simply the probability of arbitrary site is occupied. Thus, the probability, w, that the cluster to which an arbitrary occupied site belongs contains exactly s site is,

$$w_s = \frac{n_s s}{\sum_s n_s s} \tag{3}$$

and thus, the average cluster size S can be calculated by the following relation

$$S = \sum_s w_s s = \frac{\sum n_s s^2}{\sum n_s s} \tag{4}$$

Definition of the average cluster size is the same for all dimensions, although n, cannot be calculated exactly in higher dimensions.[24]

Now, to show that below p_c, pyranine intensity is proportional to S, let N_p be the number of pyranine molecules and N_m the other molecules in the lattice. Thus, the total lattice site, N is equal to $N_p + N_m$. The probability, P_p, that an arbitrary site is a pyranine molecule is N_p/N. The probability, P_y, that an arbitrary site both is a pyranine and belongs to the s-cluster can be calculated as a product of w_s and P_p as follow

$$P_y = P_p w_s = \frac{P_p n_s s}{\sum n_s s} \tag{5}$$

Thus, the total number of pyranine molecules in the clusters including s sites will be $P_y s$. The total fluorescence intensity, I, which is proportional to the total number of pyranines trapped in the finite clusters, can be calculated as a summation over all s-clusters

$$I \sim \sum_s P_y s = \sum_s \frac{P_p n_s s}{\sum n_s s} s = \frac{\sum P_p n_s s^2}{\sum n_s s} \tag{6}$$

where P_p can be taken out of the summation since the concentration of the pyranine is fixed for our work.

$$I \sim P_p \frac{\sum n_s s^2}{\sum n_s s} = P_p S \tag{7}$$

Thus, the last expression shows that the total normalized fluorescent intensity is proportional to the average cluster size. Note that the proportionality factor, P_p, is simply the concentration of the pyranine molecules in the sample cell (or the number of pyranines in the lattice). Intensity will be linearly proportional to the average cluster size, provided that the pyranine concentration is not so high to quench the fluorescence intensity by reabsorbtion mechanism and no other parameter like viscosity influencing the fluorescence intensity in addition to the concentration of pyranine.

EXPERIMENTAL

ι-carrageenan (Sigma C-1138) and pyranine (8-Hydroxypyrene-1,3,6-trisulfonic acid trisodium salt, Fluka 56360) were dissolved in $CaCl_2$ solution (0.4%) at the desired concentration by heating. Pyranine concentration was taken as 2×10^{-4} M for all samples. The heated concentration was held at 90°C and was continuously stirred by magnetic stirrer. The iota carrageenan contents were varied from 1 to 4%. These samples are named as IC1, IC15, IC2, IC25, IC3, and IC4. The compositions of the studied solutions in various ι-carrageenan concentrations are presented in Table I. The pyranine concentration was kept at 2×10^{-4} M.

The fluorescence intensity measurements were carried out using the Varian Cary Eclipse Fluorescence Spectrophotometer equipped with temperature controller. Pyranine was excited at 325 nm during *in situ* experiments and variation in the fluorescence intensity was monitored at 515 nm as a function of temperature.

Thermal phase transitions were performed in a $1 \times 1 \times 4.5$ cm^3 glass cell equipped with a heat reservoir. Before measurements, the sample was melted and then cooled to ambient temperature so that the sample in the glass cell was distributed uniformly. Then the ι-carrageenan gel was reheated up to 98°C with scan rate 0.65°C/min to obtain the gel–sol transition. Cooling of the carrageenan sol from 98°C to 20°C was then performed at the same rate to detect the sol–gel transition. Both scattered, I_{sc}, and fluorescence intensities, I_p, were monitored against temperature.

RESULTS AND DISCUSSION

The temperature dependence of the fluorescence intensities, I_p, between 20°C and 98°C are plotted in Figure 1 for the samples IC25, IC3, and IC4. It is seen that fluorescence intensities, I_p, first decreased upon heating, indicating that low temperature transition takes place. Further heating causes a dramatic increase in I_p for all samples, predicting high temperature transition.

When the carrageenan samples were cooled, the fluorescence intensity, I_p, first decreased dramatically presenting that the high temperature back transition

TABLE I
Transition Temperatures of the Studied ι-Carrageenan at Various Compositions

Samples	ι-Carrageenan (wt %)	$T_{dh} \pm 0.5$ (°C)	$T_{hc} \pm 0.5$ (°C)	$T_{ch} \pm 0.5$ (°C)	$T_{hd} \pm 0.5$ (°C)
IC1	1	46.7	–	–	25.2
IC15	1.5	50.1	–	83.3	27.7
IC2	2	51.4	84.1	82.1	30.3
IC25	2.5	54.1	84.5	80.8	31.0
IC3	3	54.8	83.7	80.9	32.9
IC4	4	52.2	82.1	80.5	35.2

occurred. Then further cooling I_p increases predicting low temperature back transition takes place. The scattered light intensities, $I_{sc,}$ were also measured and presented in Figure 2 for the samples IC25, IC3, and IC4 where it is seen that the scattered light intensity first decreased during heating and then increased. During cooling almost similar back process has presented by showing hysteresis on I_{sc} intensity.

To elaborate the above results; the observed fluorescence intensity, $I_{p,}$ has to be corrected by taking into account the behavior of scattered light intensity, to produce the real change in the fluorescence intensity due to environmental variations, i.e., thermal phase transitions. The corrected fluorescence intensity, $I,$ can be obtained from the I_p/I_k ratio where I_k acts like a light source and assume to behave like $1/I_{sc}$. Since the turbidity of the gel varies during phase transitions, one has to produce the corrected fluorescence intensity, $I,$ to eliminate the effect of physical appearance of the gel and to obtain the meaningful results for the fluorescence quenching mechanisms. Here, the observed fluorescence intensity, $I_{p,}$ is in fact the convolution of the exciting light intensity, $I_{k,}$

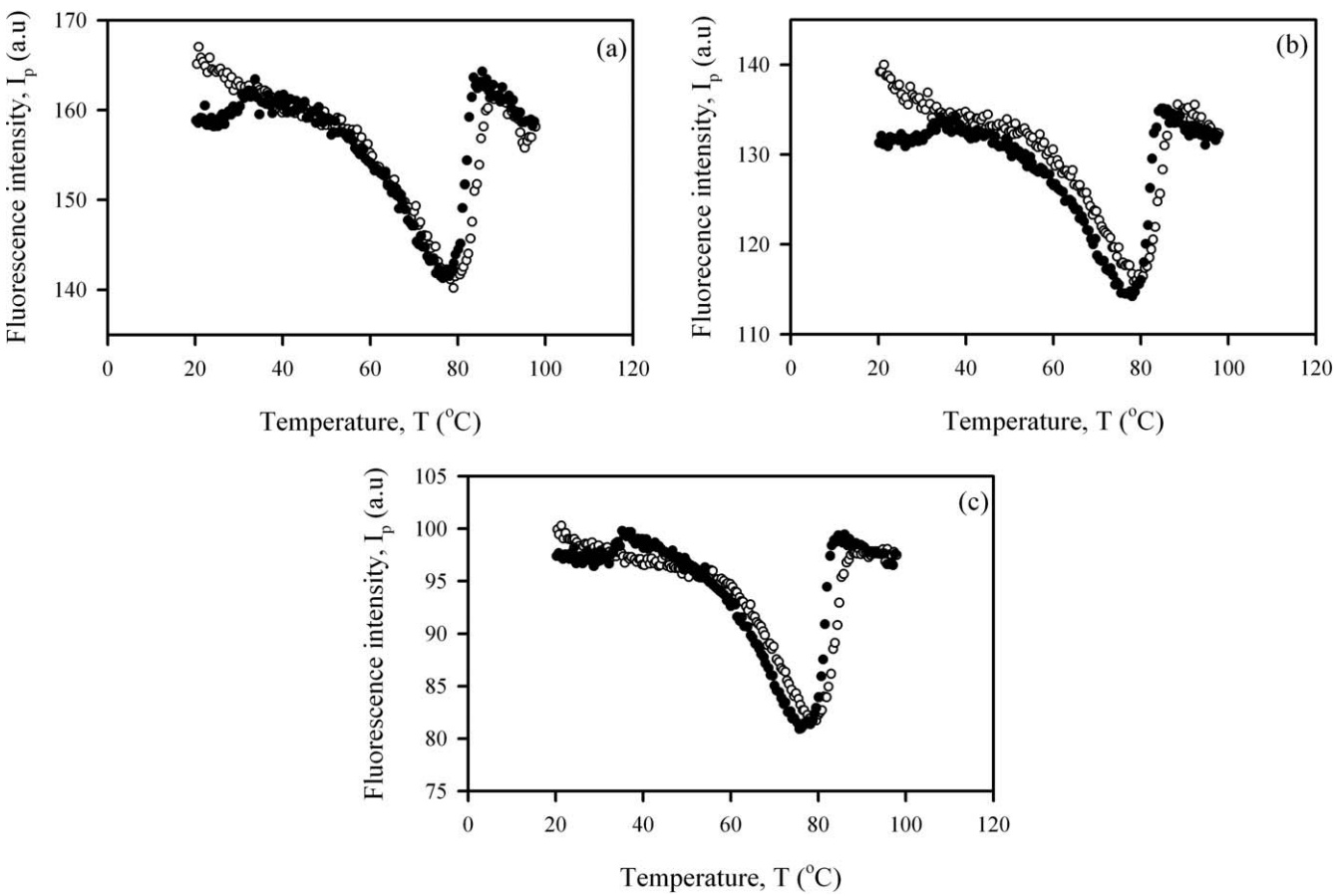

Figure 1 Temperature variation of the fluorescence intensity, I_p, for the (a) IC25, (b) IC3, and (c) IC4 samples. The heating and cooling runs are represented by open and closed circles.

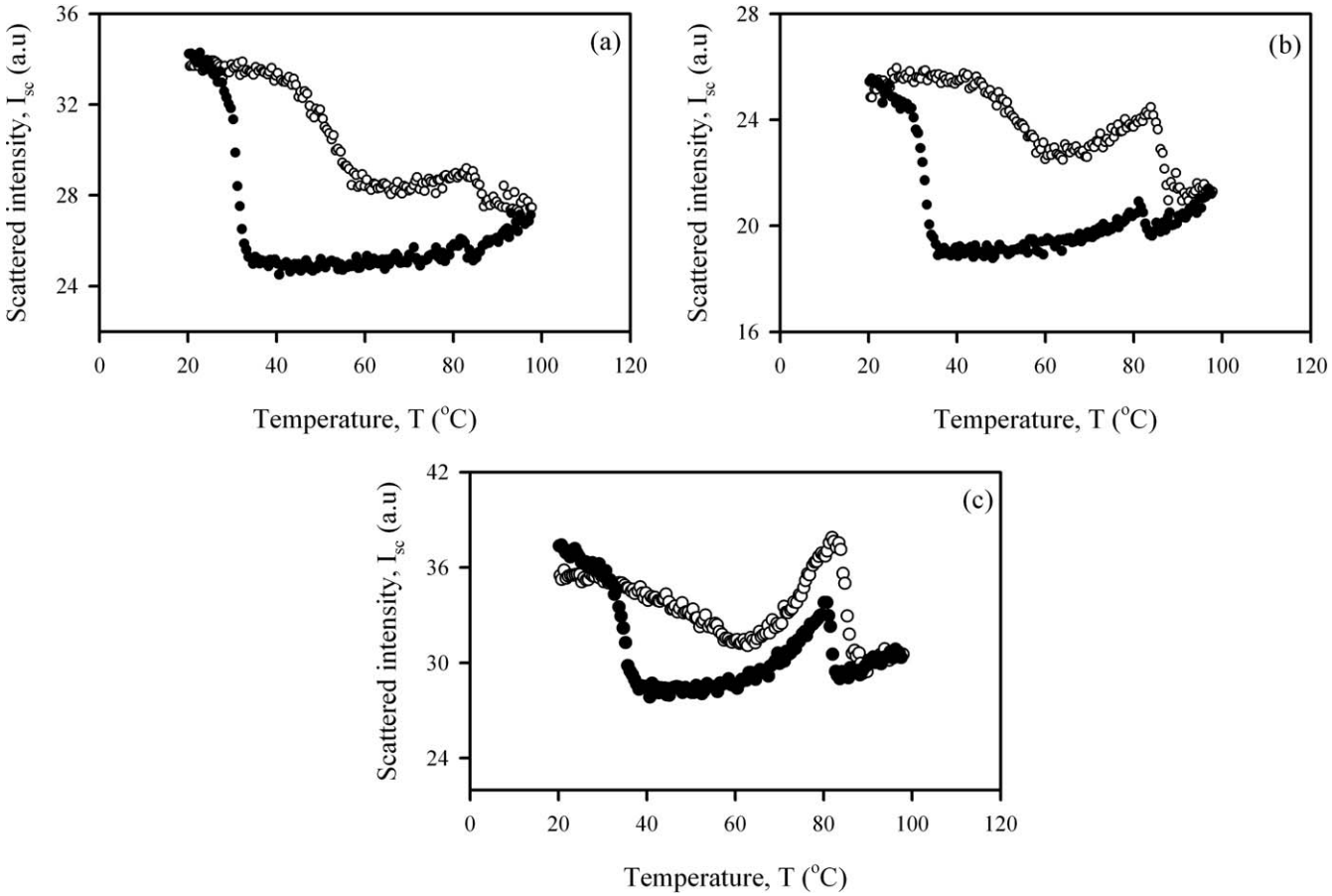

Figure 2 Temperature variation of the scattered intensity, I_{sc}, for the (a) IC25, (b) IC3, and (c) IC4 samples. The heating and cooling runs are represented by open and closed circles.

and the desired fluorescence intensity (corrected intensity, I) from the excited pyranine, where it is assumed that I_k is inversely proportional to the scattered light intensity, I_{sc}. Figure 3 presents the corrected fluorescence intensity, I, for IC25, IC3, and IC4 samples.

These results can be interpreted via Domain model proposed by some authors.[8,32] According to this model, there are two levels of ordering of ι- carrageenan in solutions and gels. These ordering can be in the form of double helix and clusters of double helices, namely dimers. This model can be explained via the following scheme,

$$[H_2]_2 \Leftrightarrow 2H_2 \Leftrightarrow 4C \quad (8)$$

where C is the random coil, H_2 is the double helix, and $[H_2]_2$ is the double helix dimer.

This model predicts high temperature transition during cooling which may correspond to the coil to double helix (c-h) transition. In other words, during the (c-h) transition, the double helix aggregate form a separate phase by excluding water from their domains as a result ι-carrageenan-water system forms two phases with different network concentrations. Quenching of excited pyranine molecules in this two phase systems has to cause decrease in the fluorescence intensity.

After the (c-h) transition, I drop to its lowest value where double helix domains are phase separated. Then system goes to the double helix to dimer (h-d) transition upon cooling where phase separated dimers form more ordered state. Increase in the corrected fluorescence intensity, I, predict more rigid environment has been reached at low temperature, which results less quenching of excited pyranine molecules in this dimer medium. When the dimers at low temperature region are heated back, then system goes into the dimer to double helix transition, where I intensity now decrease slowly back to its minima. The behavior of I during heating presented perfect hysteresis path, by showing quenching during the dimer to double helix (d-h) transition.

Upon further heating, the double helices are disappeared to the coils and system goes into the double helix to coil (h-c) transition. During (h-c) transition, increase in I can be explained by less quenching of pyranine molecules due to coiled environment.

The hysteresis at low temperature transitions can be explained by the energetic needs of (h-d) and

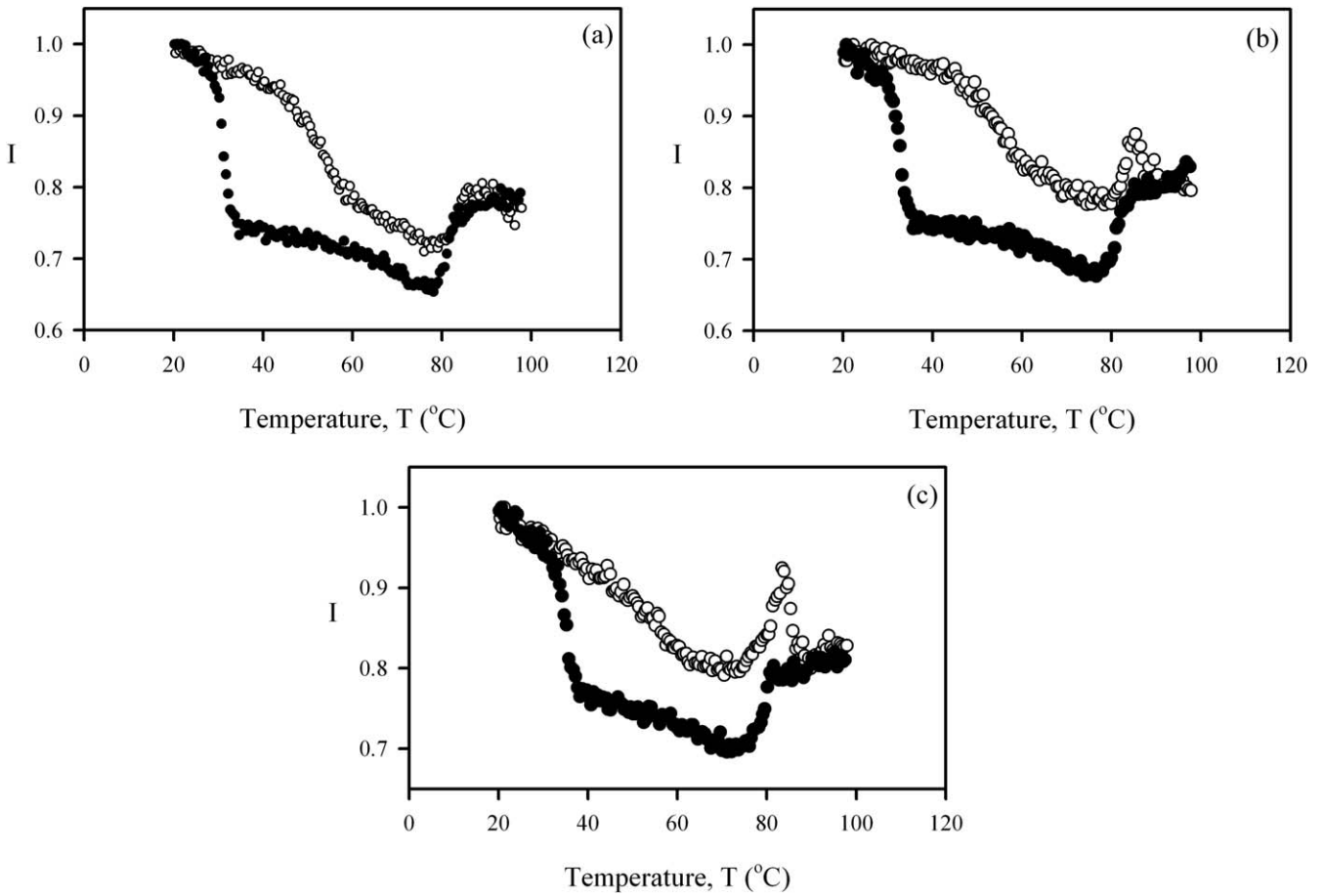

Figure 3 Temperature variation of the corrected fluorescence intensity, *I*, for the (a) IC25, (b) IC3, and (c) IC4 samples. The heating and cooling runs are represented by open and closed circles.

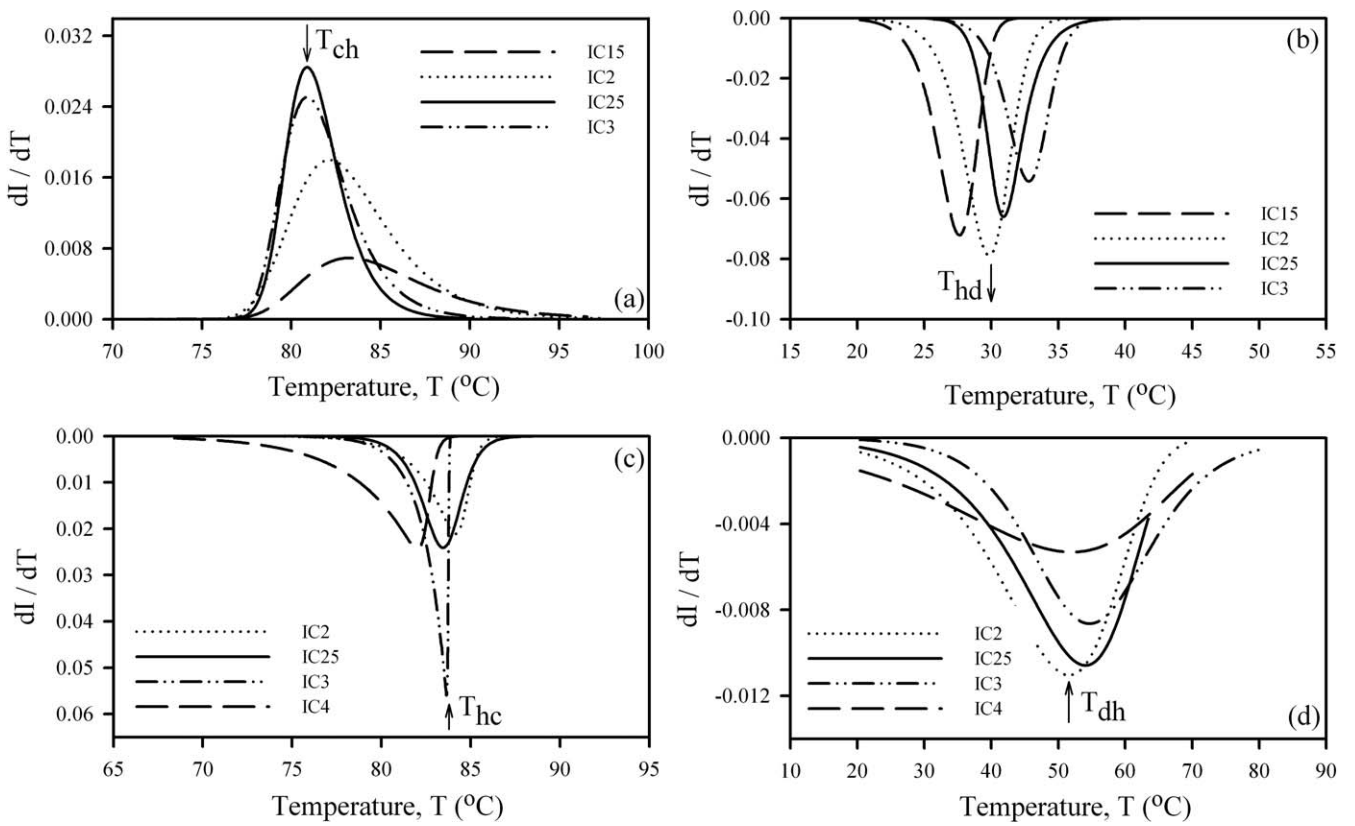

Figure 4 The first derivative of *I* curves versus temperature upon cooling for the investigated samples. The peak positions corresponded to the (a) coil to double helix, T_{ch} and (b) double helix to dimer, T_{hd} (c) double helix to coil, T_{hc} and (d) dimer to double helix, T_{dh} transitions.

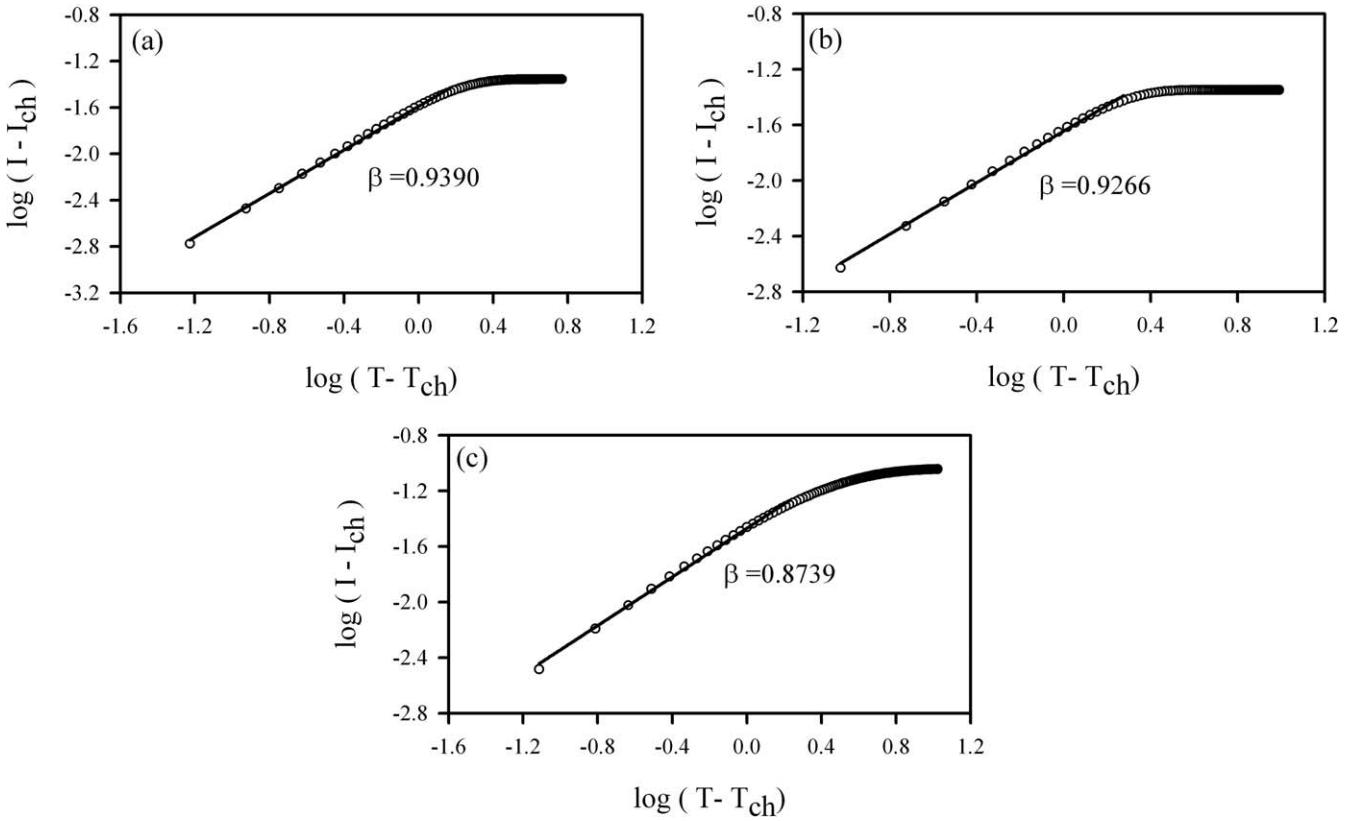

Figure 5 Log–log plots of the data near the coil to double helix transition for the (a) IC25, (b) IC3, and (c) IC4 samples.

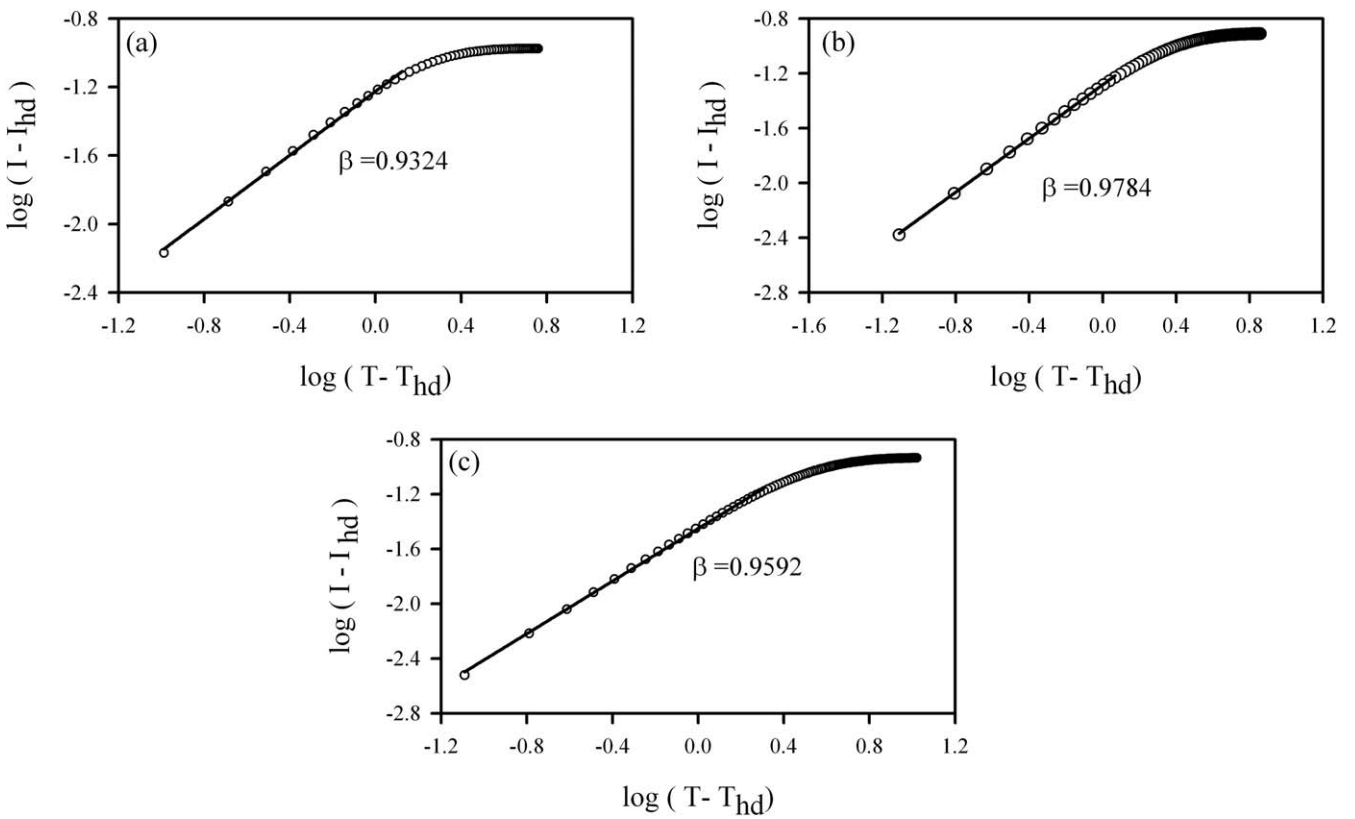

Figure 6 Log–log plots of the data near the double helix to dimer transition for the (a) IC25, (b) IC3, and (c) IC4 samples.

TABLE II
The Critical Exponents, β Near the c-h and h-d Transition for the Investigated Samples

	Coil to double helix transition	Double helix to dimer transition
Samples	β_{ch}	β_{hd}
IC1	–	0.9489 ± 0.0074
IC15	0.9335 ± 0.0061	0.9582 ± 0.0068
IC2	0.9327 ± 0.0078	0.9199 ± 0.0101
IC25	0.9390 ± 0.0093	0.9324 ± 0.0127
IC3	0.9266 ± 0.0121	0.9784 ± 0.0053
IC4	0.8739 ± 0.0107	0.9592 ± 0.0064

(d-h) transition. The (h-d) transition requires much lower energy than the (d-h) transition. That is because, formation of dimers from helices needs less energy than their dissolution.

The coil to double helix transition temperatures, T_{ch} and the double helix to dimer transition temperatures, T_{hd} were determined from the peak positions of the first derivative of I with respect to temperature. Similarly, the dimer to double helix (T_{dh}) and double helix to coil (T_{hc}) transition temperatures were also determined from the first derivative of the I curves upon heating. The measured transition temperatures which are shown in Figure 4 are listed in Table I.

It is seen in Table I that carrageenan concentration does not have significant impact on (c-h) and (h-c) transitions. On the other hand, the (h-d) and (d-h) transitions are affected by the carrageenan content. In other words, packing of helices and dimers increases the T_{hd} and T_{dh} transition temperatures.

According to Stauffer, the conversion factor p determines the behavior of the gelation process where p may depend on the temperature.[23] It can be assumed that in the critical region, i.e., around the critical point p_c that $|p - p_c|$ is linearly proportional to the $|T - T_c|$ where T_c is the critical transition temperature. For $T < T_c$, the corrected fluorescence intensity, I, measure the gel fraction, G, and can be written as a power law near the coil to double helix and double helix to dimer transitions.

$$|I - I_c| = A|T - T_c|^{\beta}, \; T \to T_c^- \tag{9}$$

where A is critical amplitude, I_c is the critical value in the transition path. The exponent β, defined in eq. (9) is established as a slope of the plot of $(I - I_c)$ versus $(T - T_c)$ on a double logarithmic scale.

The double logarithmic plots of the data for the (c-h) and (h-d) transitions are presented in Figures 5

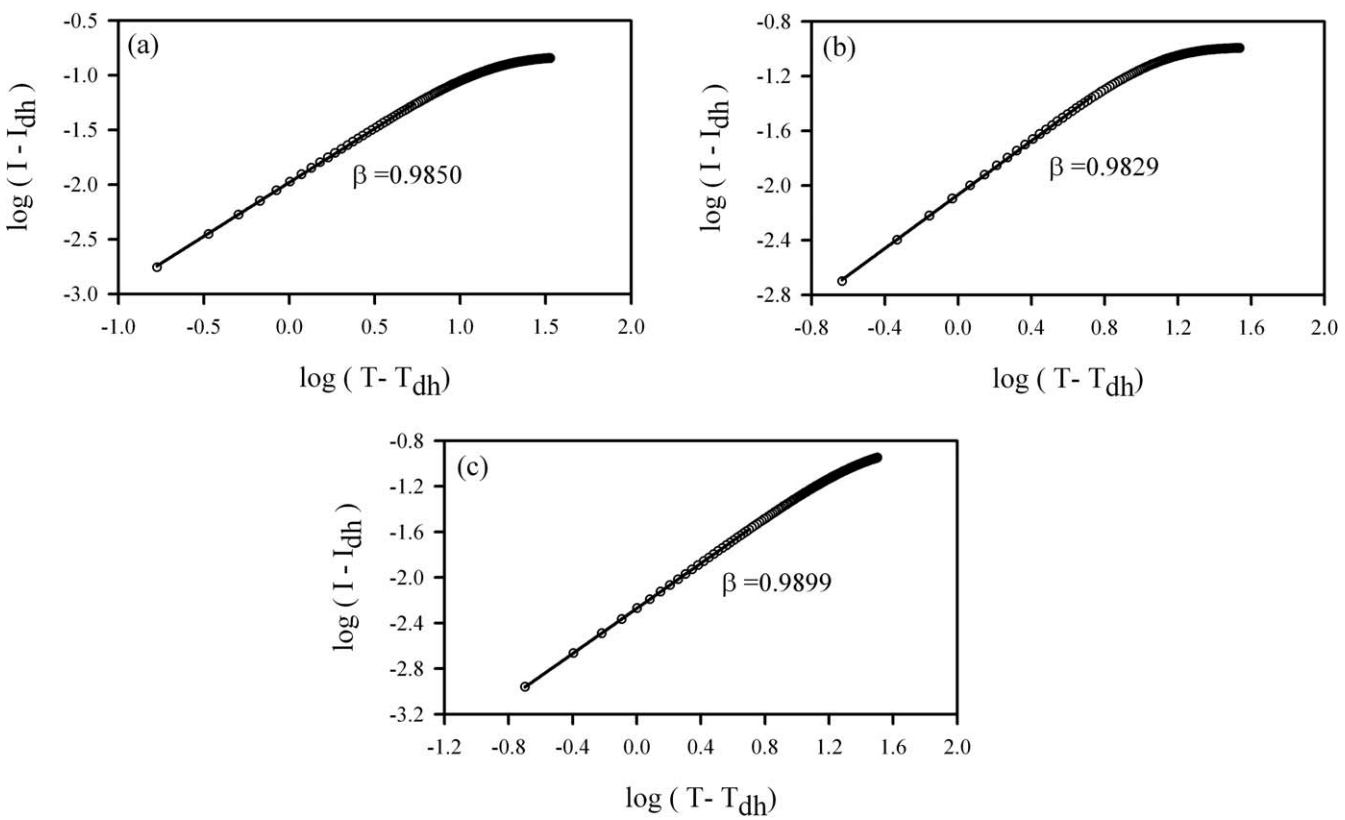

Figure 7 Log–log plots of the data near the dimer to double helix transition for the (a) IC25, (b) IC3, and (c) IC4 samples.

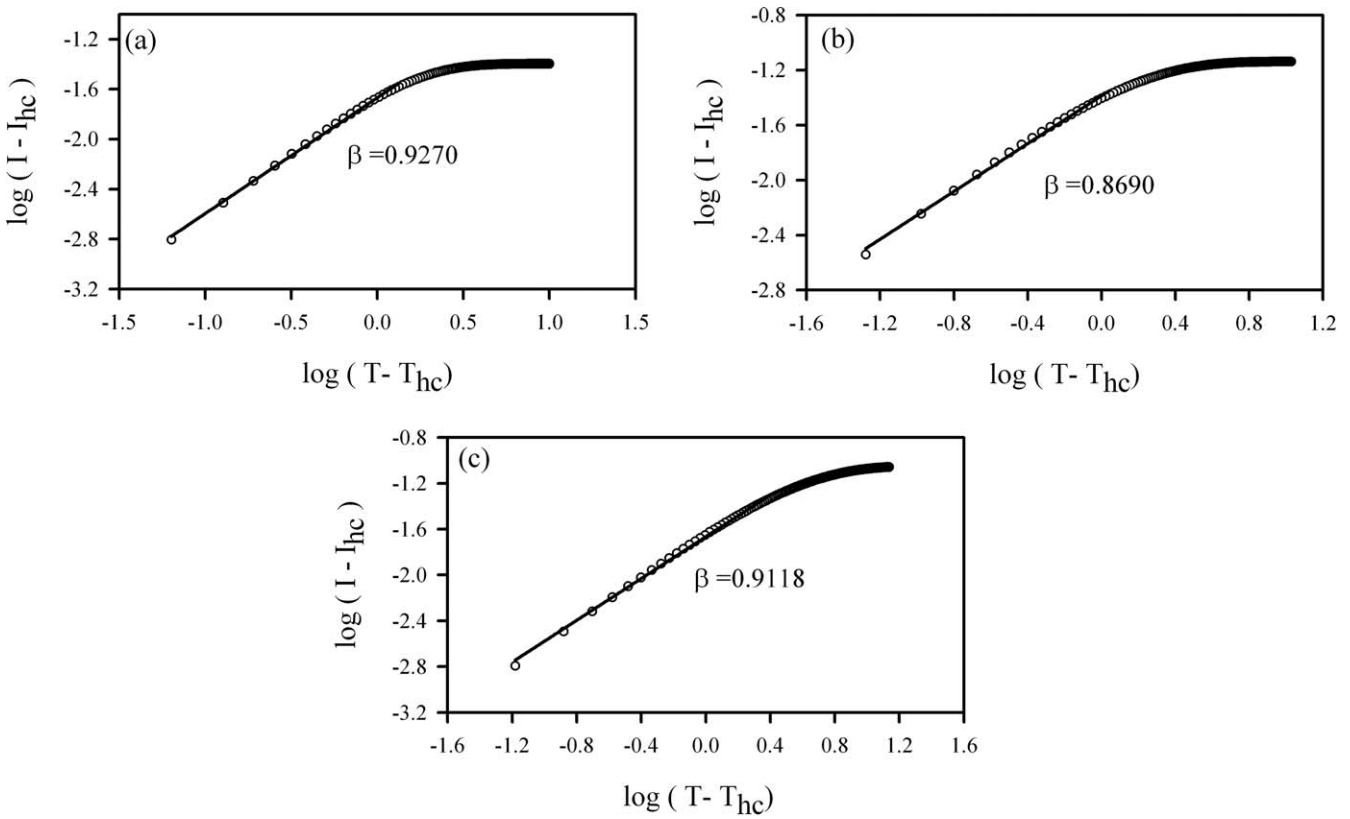

Figure 8 Log–log plots of the data near the double helix to coil transition for the (a) IC25, (b) IC3, and (c) IC4 samples.

TABLE III
The Critical Exponents, β Near the d-h and h-c Transition for the Investigated Samples

	Dimer to double helix transition	Double helix to coil transition
Samples	β_{dh}	β_{hc}
IC1	0.9615 ± 0.0052	–
IC15	0.9706 ± 0.0046	–
IC2	0.9865 ± 0.0026	0.9090 ± 0.0110
IC25	0.9850 ± 0.0027	0.9270 ± 0.0098
IC3	0.9829 ± 0.0032	0.8690 ± 0.0120
IC4	0.9899 ± 0.0004	0.9118 ± 0.0079

and 6 for the IC25, IC3, and IC4 samples where $T_c = T_{ch}$ and $I_c = I_{ch}$ are taken for (c-h) and $T_c = T_{hd}$ and $I_c = I_{hd}$ for the (h-d) transitions. I_{ch} is the critical value of intensity at T_{ch} and I_{hd} is the critical value of intensity at T_{hd}. Table II presents the critical exponents near the (c-h) and (h-d) transitions for all samples.

The critical exponents during the dimer to double helix and double helix to coil transitions upon heating can also be calculated by taking log–log plots of data at these transitions (Figs. 7 and 8). The slope of the straight lines produces critical exponent β, which are listed in Table III for dimer to double helix and

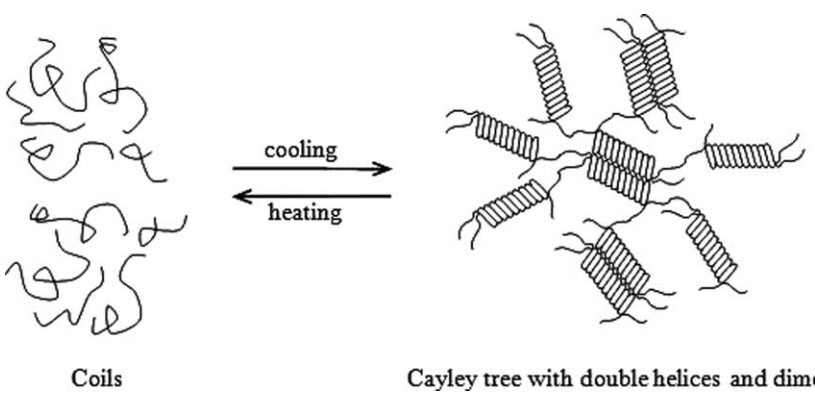

Figure 9 Cartoon presentation of the thermal phase transition according to the classical approach where the formation of Cayley tree is shown.

double helix to coil transitions. Critical exponents produced at various iota carrageenan concentrations were found to be independent of the carrageenan content. The critical exponents, β, which are listed in Tables II and III, give the average β (0.9428) value which is very close to the value of the classical Flory-Stockmayer model ($\beta = 1$).

In conclusion, sol–gel transitions from coil to double helix and double helix to dimer in iota carrageenan system obey the classical Bethe lattice model, which is now presented in Cayley tree form as shown in Figure 9. Gel–sol back transitions such as double helix to coil and dimer to double helix also follow the classical Flory-Stockmayer model.

References

1. Guo, J. H.; Skinner, G. W.; Harcum, W. W.; Barnum, P. E. J Pharm Sci Technol 1998, 1, 254.
2. Tye, R. J. Carbohyd Polym 1989, 10, 259.
3. Paoletti, S.; Smidsrod, O.; Grasdalen, H. Biopolymers 1984, 23, 1771.
4. Anderson, N. S.; Campbell, J. W.; Harding, M. M.; Rees, D. A.; Samuel, J. W. J Mol Biol 1969, 45, 85.
5. Arnott, S.; Scott, W.; Rees, D. A.; Mc Nab, C. G. J Mol Biol 1974, 90, 253.
6. Lee, I. Polymer (Korea) 1997, 21, 539.
7. Rees, D. A.; Williamson, F. B.; Frangou, S. A.; Morris, E. R. Eur J Biochem 1982, 122, 71.
8. Morris, E. R.; Rees, D. A.; Robinson, G. J. J Mol Biol 1980, 138, 349.
9. Austen, K. R. J.; Goodall, D. M.; Norton, I. T. Carbohyd Res 1985, 140, 251.
10. Norton, I. T.; Goodall, D. M.; Morris, E. R.; Rees, D. A. J Chem Soc Faraday Trans 1983, 179, 2501.
11. Kusukawa, N.; Ostrovosky, M. V.; Garner, M. M. Electrophoresis 1999, 20, 1455.
12. Lai, V. M. F.; Huang, A. L.; Lii, C. Y. Food Hydrocolloids 1999, 13, 409.
13. Norton, I. T.; Jarvis, D. A.; Foster, T. J. Int J Biol Macromol 1999, 26, 255.
14. Mohammed, Z. H.; Hember, M. W. N.; Richardson, R. K.; Morris, E. R. Carbohydr Polym 1998, 36, 15.
15. Hugerth, A.; Nilsson, S.; Sundelöf, L. O. Int J Biol Macromol 1999, 26, 69.
16. Lai, V. M. F.; Wong, P. A. L.; Lii, C. Y. J Food Sci 2000, 65, 1332.
17. Kara, S.; Tamerler, C.; Bermek, H.; Pekcan, Ö. Int J Biol Macromol 2003, 31, 177.
18. Kara, S.; Tamerler, C.; Bermek, H.; Pekcan, Ö. J Bioact Compat Polym 2003, 18, 33.
19. Pekcan, Ö.; Tari, Ö. Phase Trans 2007, 80, 799.
20. Pekcan, Ö.; Tari, Ö. Polym Bull 2008, 60, 569.
21. Flory, P. J. J Am Chem Soc 1941, 63, 3083.
22. Stockmayer, W. H. J Chem Phys 1943, 11, 45.
23. Stauffer, D.; Coniglio, A.; Adam, M. Adv Polym Sci 1982, 44, 103.
24. Stauffer, D. Introduction to Percolation Theory; Taylor and Francis: London, 1985.
25. Sahimi, M. Application of Percolation Theory; Taylor and Francis: London, 1994.
26. Adam, M.; Lairez, D.; Karpasas, M.; Gottlieb, M. Macromolecules 1997, 30, 5920.
27. Hermann, H. J. Phys Rep 1986, 136, 153.
28. Liu, Y.; Pandey, R. B. J Chem Phys 1996, 105, 825.
29. Pandey, R. B.; Liu, Y. J Sol Gel Sci Technol 1999, 15, 147.
30. Birks, J. B. Photophysics of Aromatic Molecules; Wiley: London, 1965.
31. Galanin, M. D. Luminescence of Molecules and Crystals; Cambridge International Science Publishing: Moscow, 1995.
32. Grinberg, V. Y.; Grinberg, N. V.; Usov, A. I.; Shusharina, N. P.; Khokhlov, A. R.; De Kruif, K. G. Biomacromolecules 2001, 2, 864.